<div align="center">

Final Report
Groundwater Modeling of the Casper Aquifer, Belvoir Ranch, Cheyenne
Ye Zhang, Assoc. Prof., Dept. of Geology & Geophysics, Univ. of Wyoming

</div>

Abstract

During groundwater model calibration, traditional inverse methods can suffer uncertainty due to the lack of knowledge of aquifer boundary conditions (BC) and geometry which must be used in developing a forward model. In this research, a novel groundwater inverse method is combined with geostatistical analysis methods to improve the accuracy of aquifer model calibration. The new method proposes a set of hybrid formulations of the hydrological state variables (hydraulic head and Darcy fluxes), which describe piecewise approximate solutions to the groundwater flow equation. The inverse method incorporates noisy observed data (i.e., thicknesses, hydraulic heads, fluxes, or flow rates) at measurement locations as a set of conditioning constraints. Given sufficient quantity and quality of the measurements, the method yields a single well-posed system of equations that can be solved efficiently with nonlinear optimization. For a confined aquifer with two-dimensional steady state ambient flow, the calibration results include aquifer thickness, hydraulic conductivities, head and flux distribution maps, therefore the relevant BC can be extracted. When combined with geostatistical techniques such as sequential Gaussian simulation (SGS) and multi-point geostatistical (MPS), uncertainties of both estimated parameters and BC can be obtained. The solutions of the methods are stable when measurement errors are increased up to +/- 10% of the respective measurement range. When error-free observed data are used to condition the inversion, the estimated thickness is within a +/- 5% error envelope surrounding the true value; when data contain increasing errors, the estimated thickness become less accurate, as expected. The method was applied to groundwater model calibration of the Casper Aquifer at Belvoir Ranch in southeastern Wyoming, where geostatistical techniques were used to generate stochastic facies and thickness realizations conditioned to site geological, geophysical, and borehole data. These realizations were then used as input to inversion with results including hydraulic conductivity of each facies and hydraulic head distributions extending to the recharge area of the Casper Aquifer outcrops. By combining geostatistics with inversion, uncertainty in all the outcomes are also quantified. To verify field application, a cross validation was carried out with excellent outcomes. Based on the characterization of aquifer parameters and boundary conditions, a three dimensional aquifer model was built and further calibrated.

1. Problem statement

To meet future water demands, the Cheyenne Board of Public Utilities (BOPU) plans to develop the Casper Aquifer at the Belvoir Ranch as a sustainable groundwater resource. Despite several prior studies that evaluate and characterize Casper groundwater at the ranch, complex site hydrogeology (i.e., the existence of faults, foldings, fracture networks, dissolution tubes, and cavities) precludes the development of a well-informed drilling plan, i.e., where municipal water supply wells should be placed and the appropriate seasonal pumping rate, duration, and well rotations. To ensure sustainable well yield, water supply wells need to tap into aquifer regions with high hydraulic conductivities that can also capture the natural recharge into the subsurface Casper Formation. However, significant uncertainty exists in our current understanding of groundwater flow in the Casper Aquifer at the Belvoir Ranch, due to several reasons: (1) aquifer hydraulic conductivity (K) distribution is highly uncertainty, which is related to the complex site

hydrostratigraphy; (2) location and rate of aquifer recharge remain uncertain; (3) aquifer boundary conditions (BC) are uncertain, e.g., at the Belvoir Ranch, the aquifer is intersected by several faults that range from impervious to flow to conductive.

2. Objectives

To develop a scientifically informed drilling program for the Casper Aquifer at the Belvoir Ranch, a study that can provide a quantitative guideline for the location and pumping condition of future water supply wells is needed. This study is aiming to integrate groundwater modeling with the existing geological and geophysical site data (including the current insights into fracture/dissolution tube distributions in the subsurface), as well as water level monitoring, recharge estimates, and dynamic well test results, to understand and quantify groundwater flow in the aquifer. A model domain for this study is defined in Figure 1, which includes both hydrostructural compartments where the majority of the data is located. It is bounded by the thrust fault to the east, Granite Springs and the associated anticline to the north, Casper outcrops to the west, and the Spottlewood Fault to the south. These geological structures serve as natural boundaries for the model, whereas this study will aim to determine their hydraulic properties and whether they are water divides or water conduits. Moreover, in consultation with Mark Stacy, our collaborator in this project, the model size will be modified by new evidence of aquifer structures. For example, a strike-slip fault north of the Granite Springs may influence aquifer behaviors at the ranch. Based on geological and geophysical data (i.e., structure deformation, seismic "bright spot", and low electrical resistivity), a subset of these sites has been identified (with potentially enhanced Casper permeability[1]. In this study, these locations will be subject to different pumping simulations for which an individual well's specific capacity (i.e., steady state pumping rate divided by the drawdown) will be calculated. A pumping program (rate, duration, well rotation) that can best capture the natural recharge into the aquifer, while achieving sustainable water yields will be determined at the end of this study.
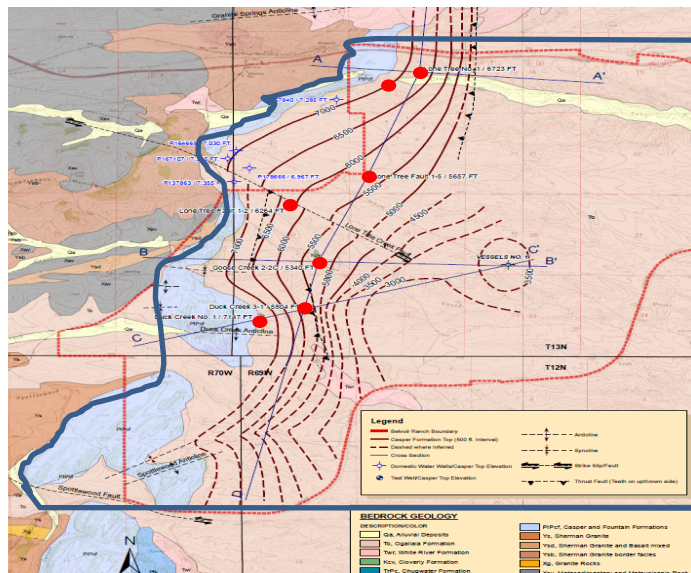
Figure 1: Study area at the Belvoir Ranch with inferred subsurface structures in the Casper Aquifer. Locations of the aquifer outcrops are shown in light blue color. Locations of four hydrostratigraphic cross sections (A-A', B-B',C-C', and D-D') are shown. The proposed modeling domain is shown by the blue outline.

3. Methodology

This study uses Petrel [2-3] to incorporate all site static data within the model domain to build a 3D hydrostratigraphic model, including the Casper Aquifer and its overlying formations. This model will incorporate both large-scale stratigraphic information (including the shape and extent of faults and fracture networks), as delineated by the seismic and resistivity data, and small-scale aquifer heterogeneity, as identified by the well logging data. Groundwater simulations will be performed with FEFLOW, whereas both the model parameters (Ks, storativities, and recharge rates) and the unknown model boundary conditions will be calibrated against the aquifer monitoring data using a hybrid inversion technique [4]. This hybrid technique has a potential to address complex and realistic aquifer problems by combining a novel steady-state inverse method developed by the PI's group [5-7] with a traditional, objective-function-based technique (PEST[7]) that can be used to fit transient data. The novel inverse method is physically-based, as it conserves the continuity of hydraulic head and groundwater fluxes throughout the aquifer, while its solution is conditioned to measurements that can also contain errors. Importantly, the novel method does not assume the knowledge of the aquifer BC, e.g., whether any of the bounding subsurface structures in the Casper Aquifer actually represents a no-flow or a flow-through boundary. Instead, the BC is obtained from the inverse solution. On the other hand, calibration techniques such as PEST require the precise knowledge of aquifer BC in order to accurately assess the model-data mismatch with a forward simulation model. However, aquifer subsurface BC are usually uncertain, as is discussed above for the Casper Aquifer. Even if additional wells are drilled all along the aquifer boundaries, such measurements will contain errors, which can significantly impact the accuracy of the traditional techniques.

4. Progress to date including significance

### 4.1 Monitoring data acquisition

From June 6th to 8th, 2016, an additional well, Lone Tree MON No. 1, was drilled and developed in Belvoir Ranch near Lone Tree Creek and is close to the existing well Lone Tree No. 1. The purpose of drilling this well is to better understand the recharge from Lone Tree Creek to Casper Aquifer. Longitute and Latitue of Lone Tree MON No. 1 are 41˚5'42.11"N and 105˚8'50.78"W, respectively. Lone Tree MON No. 1 is located between the Lone Tree Creek Sink and Lone Tree No.1. Lone Tree compartment is the most productive compartment according to pumping project. Monitoring water level data from this well will contribute to the estimation and verification of recharge rate from Lone Tree Creek to Casper Aquifer. This well has 2-in diameter, and total depth is 177 feet. The measured water level is 46.18 feet from top of casing after well completion and development. Moreover, since summer, 2016, all seven observation wells were instrumented. Water level data have been measured every thirty minutes from each of the well. These head data are then sent by the telemetry system to the server. Water level data from summer of 2016 to the most recent date has been plotted with snow depth data from nearby SNOTEL and snow stations (Figure 2). Water level data will be used for parameter and boundary condition estimation.

Figure 2: Plotted water level data with snow depth data
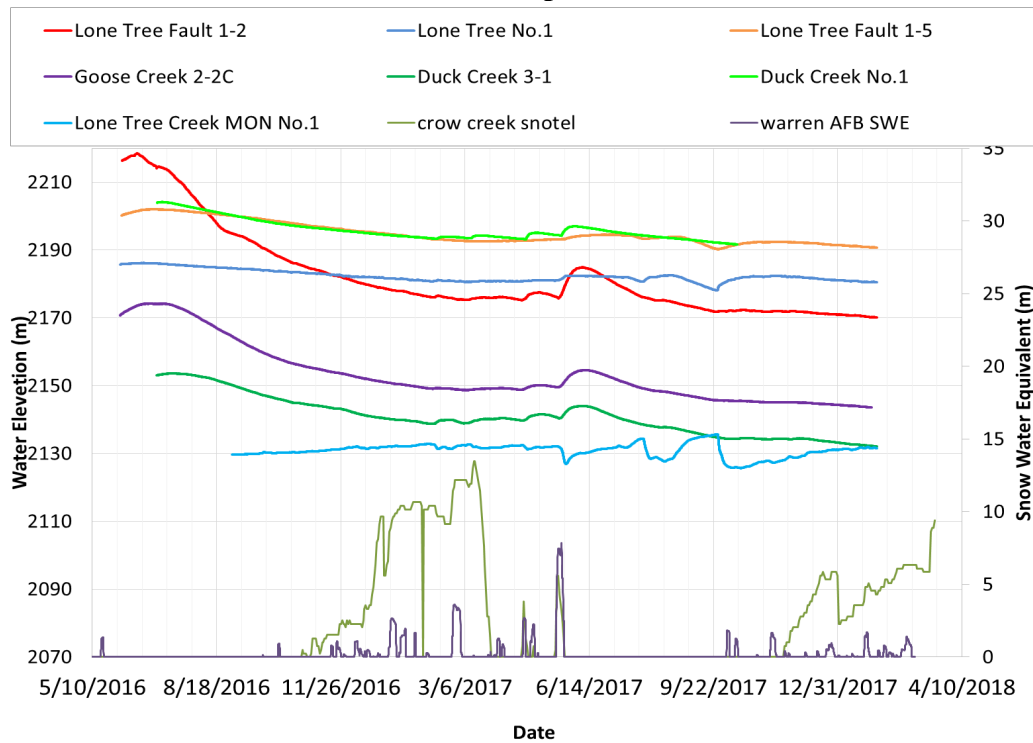
4.2 Aquifer structural model
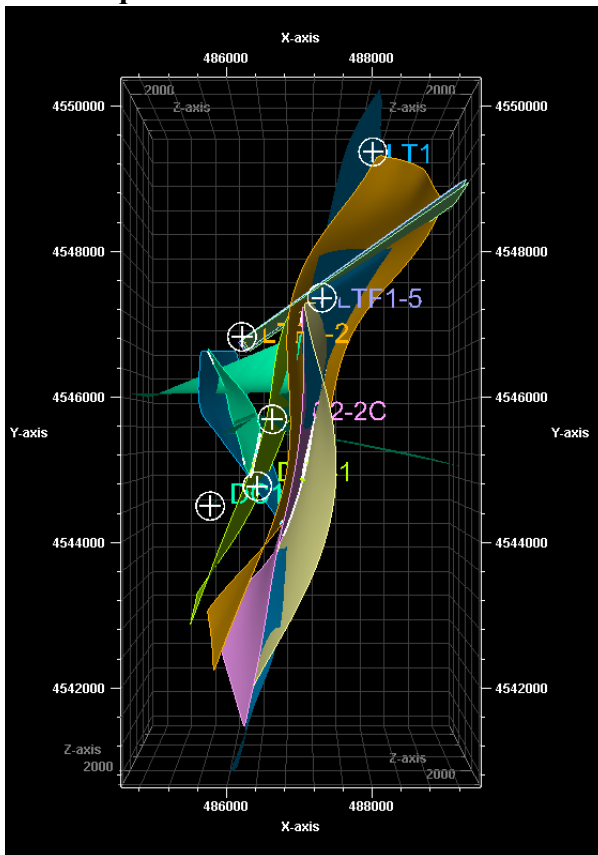
Static model has been built with Petrel by integrating the observed static aquifer structure data, including hydrostratigraphy, faults, as obtained from geological, geophysical, and logs. 2D seismic geophysical data was the soft data used to initially build the draft 3D model. Five interpreted lines from Zonge Inc. were provided [1], and then formation tops for Chugwater Formation, Goose Egg Formation, Upper Casper Formation, and Lower Casper Formation were interpreted and generated in Petrel. Locations of the faults were also interpreted from the 2D seismic data. Figure 3 is the draft fault model created with Petrel from last year's annual report.

Figure 3: Fault model created by Petrel in 2016 which is showing the interpreted faults in the site area.

In 2017, a preliminary Petrel model was built to incorporate the three essential faults shown on the geologic map. The model built in 2016 with very complex fault system only captures two of the three essential faults shown on the geologic map.
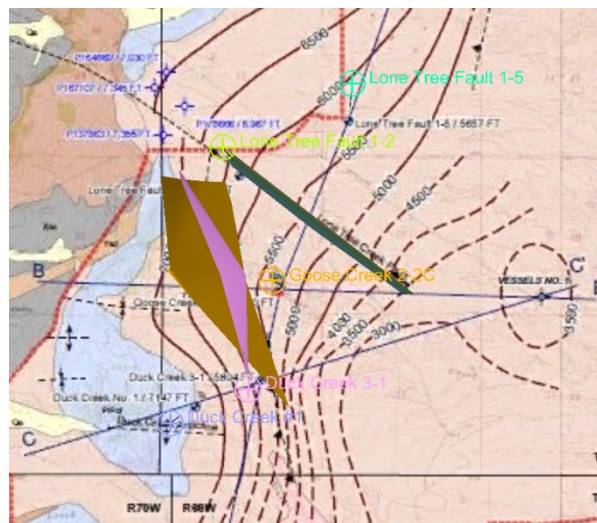
Including all interpreted faults from seismic data is not necessarily the optimized option. Indeed, the model with three faults is a good candidate to start with since these three faults are proved both by surface geology and seismic interpretation.

The Petrel model is also rebuilt with the seismic cross sections in depth domain instead of time domain, so all of the depth units are consistent with each other. The horizons (top and bottom of each formation) of Petrel model are also reinterpreted, thus the resulted surfaces are smoother. Surfaces are cleaned based on geologic map and depositional order. The updated model is shown in Figure 4(a), and the comparison between the geologic map and the updated fault model is shown in Figure 4(b).

**Figure 4: Updated Fault model created by Petrel showing three essential faults in the site area.**

b. Comparison between the geologic map and the updated fault model
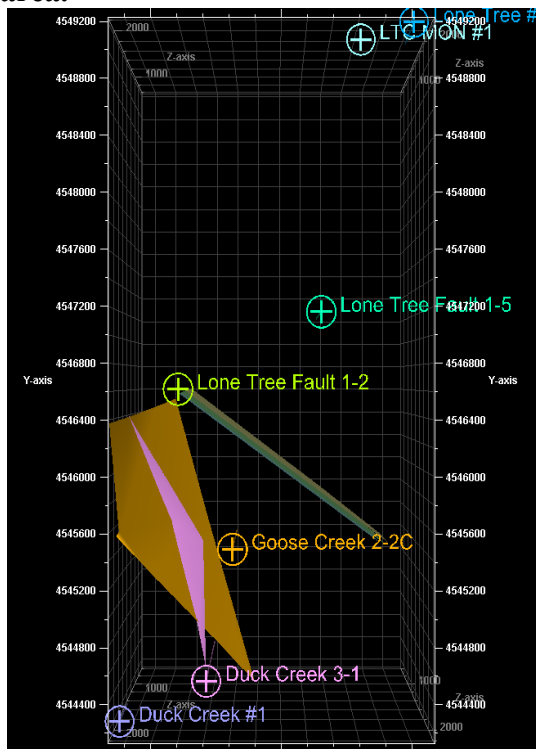
a. Updated Petrel fault model

Bird's view map of each formation is shown in Figure 4. In this updated model, six horizons are made. First horizon is the surface excluding Casper Aquifer outcrop; second horizon is the bottom of either White River or Ogallala Formation, since they are the erosional formations; third horizon is top of Chugwater Formation; fourth horizon is top of Goose Egg Formation; Fifth horizon is top of Casper Aquifer, and compare to the previous model, Upper and Lower Casper formations are combined to Casper Formation for preliminary simulation; and the sixth horizon is top of Sherman Granite.

Figure 5: Bird's view map of each surface.
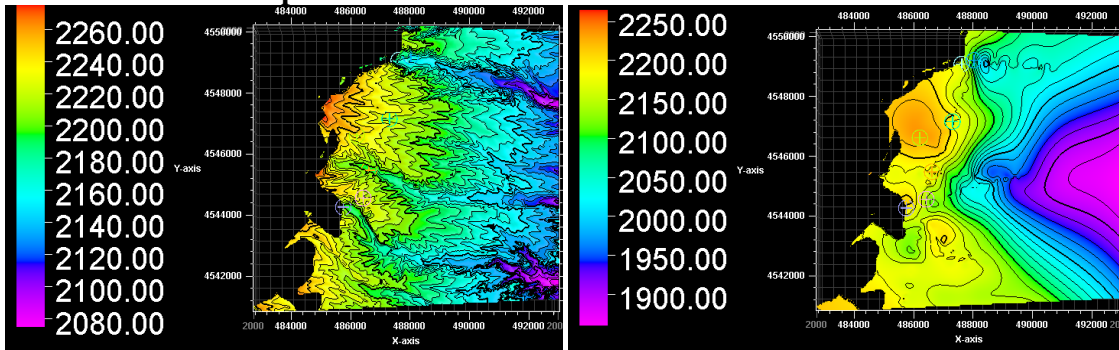
Surface excluding
Casper Aquifer outcrop

Bottom of White River
and Ogallala Formation
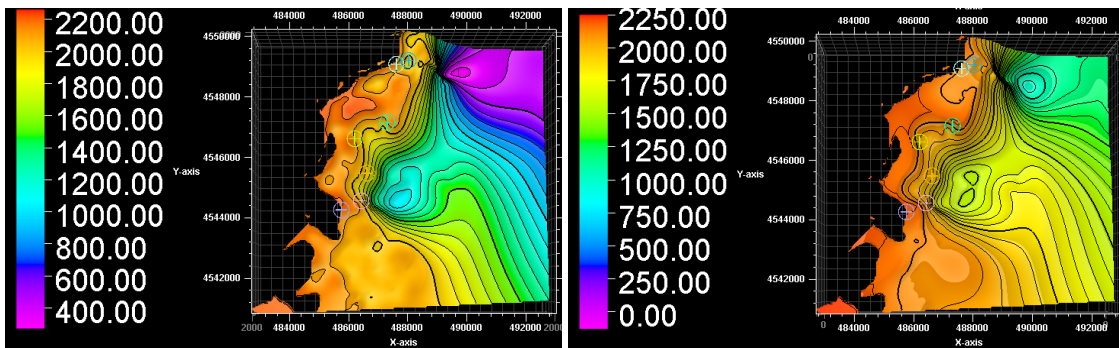
Top of Goose Egg
Formation

Top of Chugwater
Formation
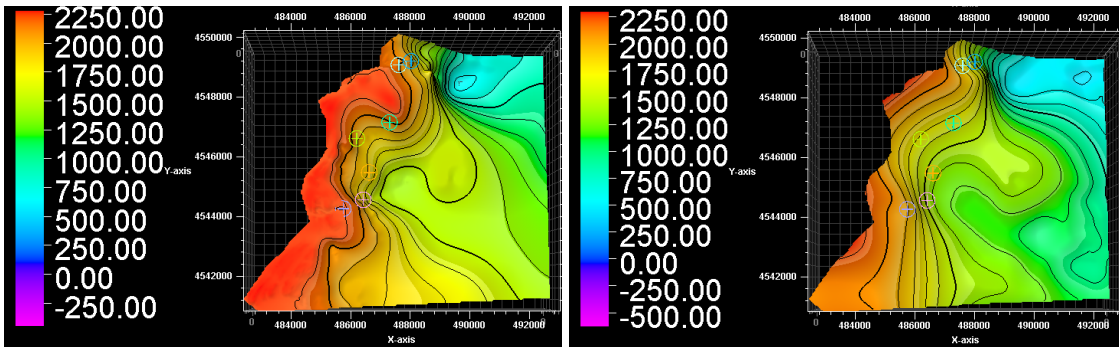
Top of Casper Aquifer

Top of Sherman Granite

The elevations of the formation tops were all verified with hard data. Figure 6 is the updated 3D integrated model with the formation tops. This Petrel static model is exported to FEFLOW for further parameter estimation work. A new inversion method developed by our group is used to estimate boundary conditions for Casper Aquifer.

Figure 6: Updated 3D Petrel model with formation tops and location of the wells.
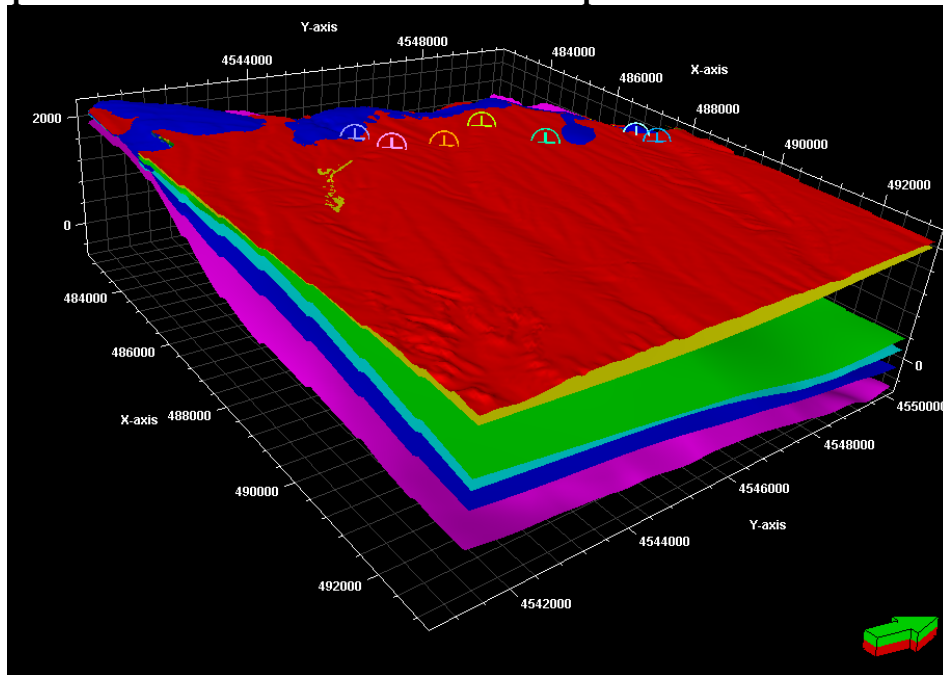

4.3 Parameter estimation

In 2016, it was proposed to use GWV for model calibration. However, after reviewing the capability of GWV, we've found that the dipping angle of Casper Aquifer is exceeding the calibration range of GWV, and it will give estimated parameters high error [7]. Thus, the model calibration work was performed using FEFLOW and FePEST instead of GWV and PEST. The Petrel structural model was imported to FEFLOW as a forward model. The FEFLOW model incorporates faults, well locations, three compartments (Lone Tree, Goose Creek, and Duck Creek), and tops of formations (Figure 7a). Finite element mesh was generated based on the locations of the geological features.

Figure 7: a. FEFLOW model with geological structures and well locations. b. Finite element mesh that incorporate geological features.
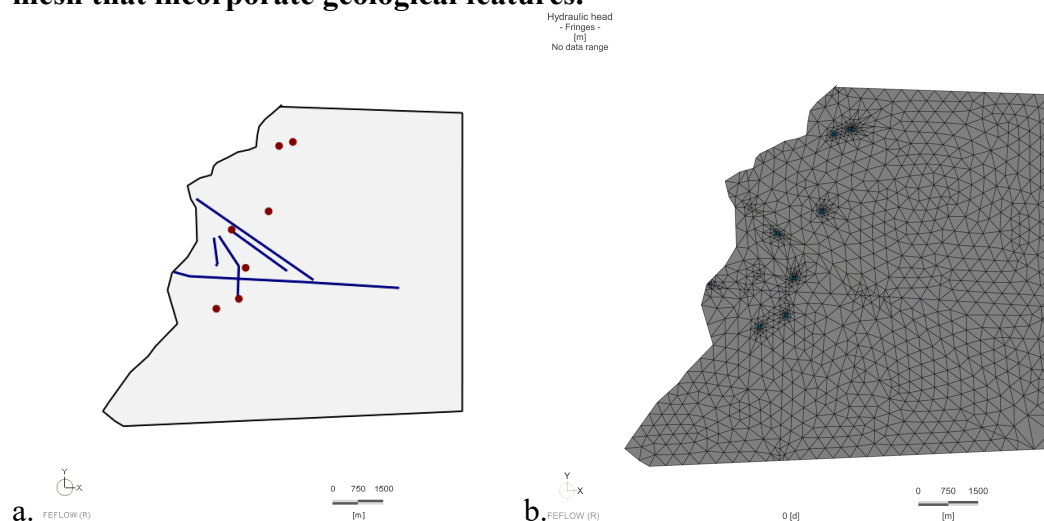
After generating the mesh, elevation data of top and bottoms of the formations were imported to FEFLOW to give a 3D hydrostatic model (Figure 8).

Figure 8: 3D FEFLOW structural model.
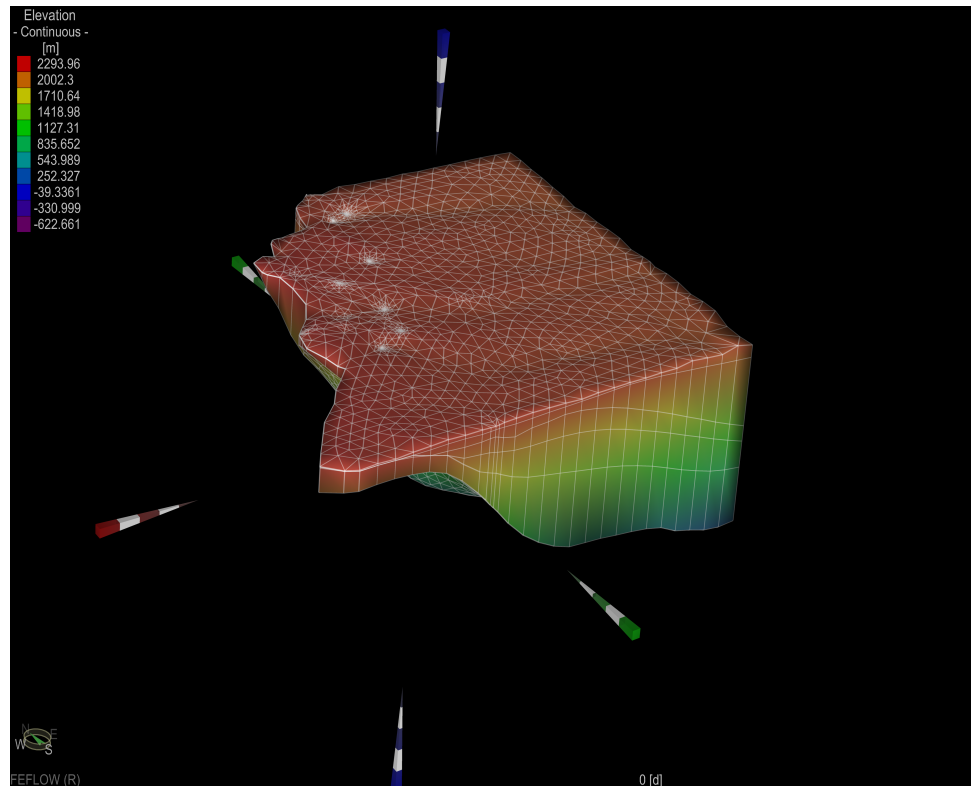
<u>Initial parameter estimations:</u>

Previously, initial hydraulic parameter estimations were from 2012 Lidstone final report [1]. The estimations had been verified by using Aqtesolv with historic pumping data. Boundary conditions were roughly assigned to the model based on water level contour map from recent monitoring well data collection.

This year, new methods were also applied for hydraulic parameter and boundary condition estimation. Point-scale hydraulic conductivity values were estimated from core cuttings and well logs. Core cuttings are available for all wells except for Lone Tree Creek MON No. 1 well. For the 6 wells with core cuttings, a point-scale K (cm/s) was estimated using (results are shown in Table 1):

$$K = \frac{\delta_w g}{\mu} \cdot \frac{d^2}{180} \cdot \frac{\phi^3}{(1-\phi)^2}$$

Where d is diameter of the grain size (cm), which can be found from the cuttings using the grain size chart, δ_w denotes the fluid density ($\frac{g}{cm^3}$), μ is dynamic viscosity ($\frac{g}{cm \cdot s}$), and g is the acceleration of gravity which is 980 ($\frac{cm}{s^2}$).

Table 1: Calculated point-scale *K* from logging and cutting data in 6 wells.

	Corrected K ($\frac{gpd}{ft^2}$)
Lone Tree Fault MON No.1	N/A
Lone Tree #1	39.5
Lone Tree Fault 1-5	71.8
Lone Tree Fault 1-2	70.1
Goose Creek 2-2C	86.1
Duck Creek 3-1	9.8
Duck Creek #1	13.5

Hydraulic conductivity data from both Lidstone final report and point-scale estimation were assigned to FEFLOW model (Figure 9a). Figure 9b shows that there are six hydraulic conductivity zones in Casper aquifer (three compartments and three fault zones).

a.   b.
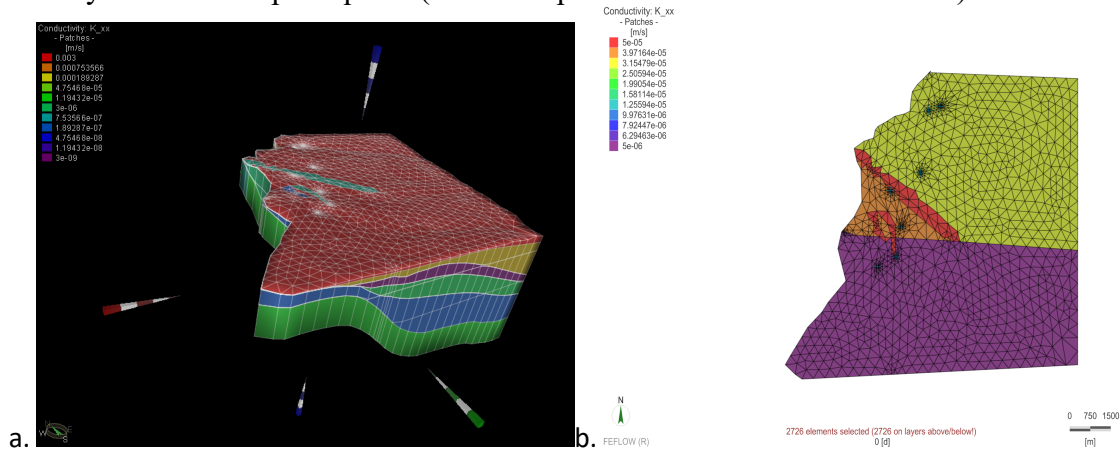
Boundary conditions of the forward model were estimated using novel inverse methods with water level measurements in 2011(Table 2).

Table 2: Water levels of 6 wells in 2011.

	Lone Tree #1	Lone Tree Fault 1-5	Lone Tree Fault 1-2	Goose Creek 2-2C	Duck Creek 3-1	Duck Creek #1	LTC MON #1
Elevation (m)	2175.7	2228.3	2246.0	2198.1	2232.5	2204.2	2160.5
2011 Depth to Water (m)	19.5	64.2	102.8	74.7	125.7	67.9	
Water Level Elevation (m)	2156.2	2164.1	2143.2	2123.4	2106.8	2136.3	

A set of fundamental solutions of inversion is fitted locally to the observed water level and hydraulic conductivity, while flow continuity is honored over all inversion grid cells. The fundamental solutions of inversion are derived by solving the steady-state groundwater flow equation to obtain a set of local analytical solutions assuming that local *K* of a subdomain or a single inversion grid cell is homogeneous. However, unlike [3], whose fundamental solutions yielded only a single *K* value (i.e., ratios between facies K s were assumed known as a setoff prior information constraints for inversion), the fundamental solutions have been modified to allow the simultaneous estimation of both *K*s of the reference model (this approach is extendable to any number of facies):

$$\tilde{h}(x, y) = a_o + a_1 x + a_2 y + a_3 xy + a_4(x^2 - y^2)$$
$$\tilde{q}_x(x, y) = -K(a_1 + a_3 y + 2a_4 x)$$
$$\tilde{q}_y(x, y) = -K(a_1 + a_3 x + 2a_4 y) \qquad (x, y) \in \Omega_i \qquad (2)$$

where $\tilde{h}$ denotes the approximate hydraulic head, $(\tilde{q}_x, \tilde{q}_y)$ denote the approximate groundwater fluxes, a_i ($i = 0,\ldots,4$) denote a set of coefficients that locally define these approximate solutions, K is local hydraulic conductivity: $K \in (K_1; K_2, \ldots)$ of the facie, and Ω_i is a subdomain of the problem, here corresponding to an inversion grid cell.

The continuity equations, which penalize the mismatch between the fundamental solutions at the interface between adjacent inversion grid cells, can be written as:

$$\delta\big(p_j(x_{,j},y_j)-\epsilon\big)\Big(K_1\,\tilde{h}^{(k)}(x,y)-K_1\,\tilde{h}^{(l)}(x,y)\Big)=0, \qquad \forall^{(k,l)}\in K_1$$

$$\delta\big(p_j(x_{,j},y_j)-\epsilon\big)\Big(K_2\,\tilde{h}^{(k)}(x,y)-K_2\,\tilde{h}^{(l)}(x,y)\Big)=0, \qquad \forall^{(k,l)}\in K_2$$

$$\delta\big(p_j(x_{,j},y_j)-\epsilon\big)\Big(K_m\,\tilde{h}^{(k)}(x,y)-K_m\,\tilde{h}^{(l)}(x,y)\Big)=0, \qquad \forall^{(k,l)}\in K_1 \in K_2 ,m \in (1,2)$$

$$\delta\big(p_j(x_{,j},y_j)-\epsilon\big)\Big(\tilde{q}_n^{(k)}(x,y)-\tilde{q}_n^{(l)}(x,y)\Big)=0, \qquad \forall\,K^{(k)} \neq K^{(l)}$$

$$\delta\big(p_j(x_{,j},y_j)-\epsilon\big)\Big(\tilde{q}_t^{(k)}(x,y)-\tilde{q}_t^{(l)}(x,y)\Big)=0, \quad \forall\,K^{(k)} \neq K^{(l)} \quad (3)$$

where $p_j(x_{,j},y_j)$ denotes the jth collocation point, which lies on the interface between grid cells (k) and (l), $\tilde{q}_n$ is normal flux at p_j, $\tilde{q}_t$ is tangential flux at p_j, $\delta\big(p_j(x_{,j},y_j)-\epsilon\big)$ is a Dirac delta weighting function [3] that samples the mismatch between the fundamental solutions at $p_j(x_{,j},y_j)$. The relation between $(\tilde{q}_n, \tilde{q}_t)$ and $(\tilde{q}_x, \tilde{q}_y)$ can be determined using the angles between the interface and the global coordinate axis.

Inversion further satisfies a set of data constraints which can be written as:

$$\delta(p_t-\epsilon)\Big(K_m\tilde{h}^{(k)}(x_t,y_t)-K_mh^o(x_t,y_t)\Big)=0, \quad m \in (1,2)$$

$$\delta(p_t-\epsilon)\Big(\tilde{h}_n^{(k)}(x_t,y_t)-h_n^o(x_t,y_t)\Big)=0$$

$$\delta(p_t-\epsilon)\Big(\widetilde{K}_n^{(k)}(x_t,y_t)-K_n^o(x_t,y_t)\Big)=0 \quad (4)$$

where $\delta(p_t-\epsilon)$ is the Dirac delta weighting function, which reflects confidence in the observed data (e.g., it can be inversely proportional to the measurement error variance), (x_t,y_t) represents the location where an observed datum was sampled, and h^o, K^o are the observations, K_m denotes the conductivity of the facies which contains the observations. If the flux measurements exist, they will be used here to provide flow rate related information for inversion because conductivity cannot be uniquely identified from hydraulic head observations alone. If subsurface flow rate measurements are available, the flux conditioning equations can be integrated to enforce conditioning by flow rates [3]. In Belvoir Ranch, neither flux or flow rate data are available, thus only head and local conductivity data were used for inversion. The inverted head map using 2011 water level data is shown in Figure 10a. The boundary conditions along the ranch boarders are assigned to FEFLOW forward model (Figure 10b).

Figure 10: a. Inverted head map using the novel inverse method. b. FEFLOW model with boundary conditions.

a.　　　　　　　　　　　　　b.
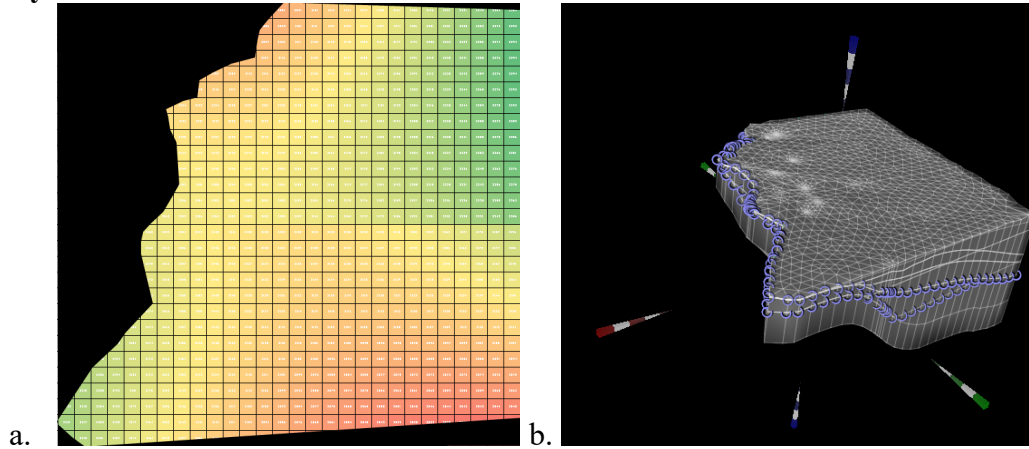
Besides boundary conditions of Belvoir Ranch, an averaged annually natural recharge rate had been assigned to the top layer of the model. According to [8], annual precipitation rate of Cheyenne is 16 inches, and about 22% of the precipitation goes into underground [9], thus a constant value of recharge rate of 2.27e-4 m/d was assigned to the Model (Figure 11).

Figure 11: A constant rate of recharge was assigned to the top layer of the model.
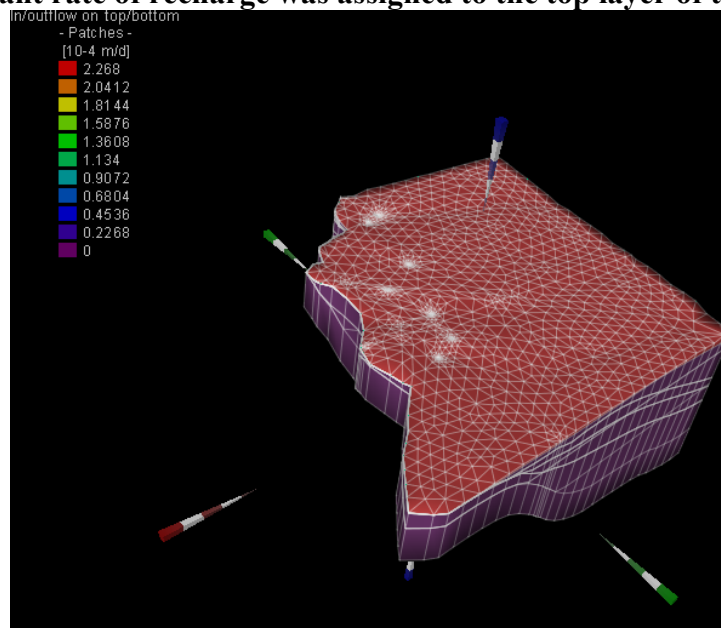
Parameter estimation with FEFLOW-PEST

In 2011, there were three pumping events in the ranch, and were performed for each compartment at a time. Water level data of the pumping well and observation wells from each of the pumping test were imported to FEFLOW for parameter estimation (Figure 12).

Figure 12: FEFLOW model of Lone Tree Creek(a), Goose Creek(b), and Duck Creek(c) compartment.

a. b. c.
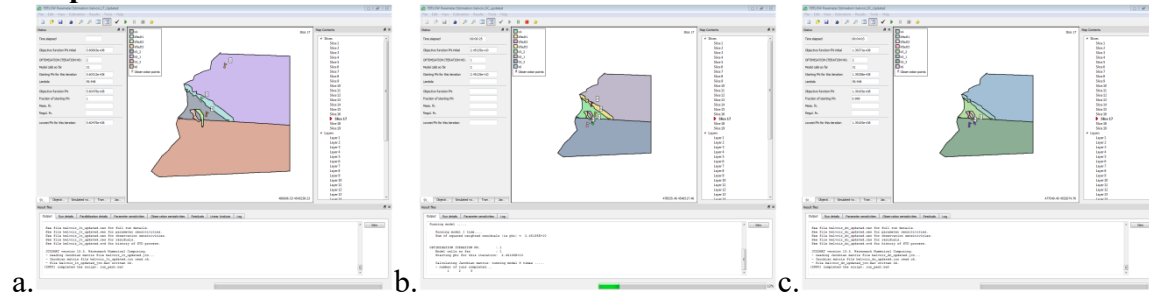
Hydraulic conductivities of Goose Egg Formation, three faults, three compartments of Casper Aquifer, and Sherman Granite were calibrated for each pumping test. The results of the three pumping test calibrations are shown in Table 3. Highlighted cells represents for the estimated values that will be used to calculate a value for an integrated model. Estimated parameters were used in a forward model for further analysis.

Table 3: FEFLOW hydraulic conductivity estimation results.

Pumping Well	Lone Tree Fault 1-5	Duck Creek 3-1	Goose Creek 2-2C	Estimated Parameters (m/s)
Observation Wells	Lone Tree No.1, Lone Tree Creek 1-2, Goose Creek 2-2C	Duck Creek No.1	Duck Creek 3-1, Lone Tree Fault 1-2, Duck Creek No.1	
Goose Egg Formation	6.18E-06	4.61E-06	1.07E-06	3.95E-06
Fault No.1	1.06E-07	1.05E-05	3.44E-05	1.06E-07
Fault No.2	1.62E-06	1.67E-06	1.96E-06	1.81E-06
Fault No.3	1.55E-06	1.58E-06	1.63E-06	1.61E-06
Lone Tree Creek Compartment	4.43E-04	3.87E-04	1.30E-04	4.43E-04
Goose Creek Compartment	1.98E-07	2.28E-06	1.44E-07	2.28E-06
Duck Creek Compartment	1.02E-07	8.09E-08	1.66E-07	1.66E-07
Sherman Granite	8.74E-06	7.55E-06	1.26E-06	5.85E-06

By incorporating geophysical and borehole data at the Ranch, a 3D aquifer model was built. Aquifer boundary conditions in April 2016, inverted using the new inverse method, were imported to the model, the assumption being that the radial cone of depression from the pumping program will not reach the actual boundaries. This assumption, however, will be subject to revision. The calibrated hydraulic conductivity values, also obtained from inversion, were assigned to the Casper Aquifer layers in the 3D model. The 3D model was first run under steady state flow with zero pumping rates for all wells. The simulated water level and observed water level are compared. The percentage errors of the simulated heads of all wells are within +/-4%.

Table 4: Comparison between simulated heads and true heads in 6 wells (Lone Tree MON #1 is a monitoring well).

	True heads (m)	Simulated heads (m)	%error
LT1	2180.8	2114.3	3.15%
LT15	2192.7	2134.8	2.71%
LT12	2176.1	2161.9	0.66%
GC22C	2149.2	2156.1	0.32%
DC31	2140.3	2156.9	0.77%
DC1	2193.9	2167.4	1.22%

4.4 Pumping Modeling

The same 3D model is run under transient mode where multilayer production wells were assigned to the six well locations (Figure 13). Since Lone Tree MON#1 is an observation well, it will not be used during production well design.

Figure 13: Multilayer wells in the FEFLOW model.
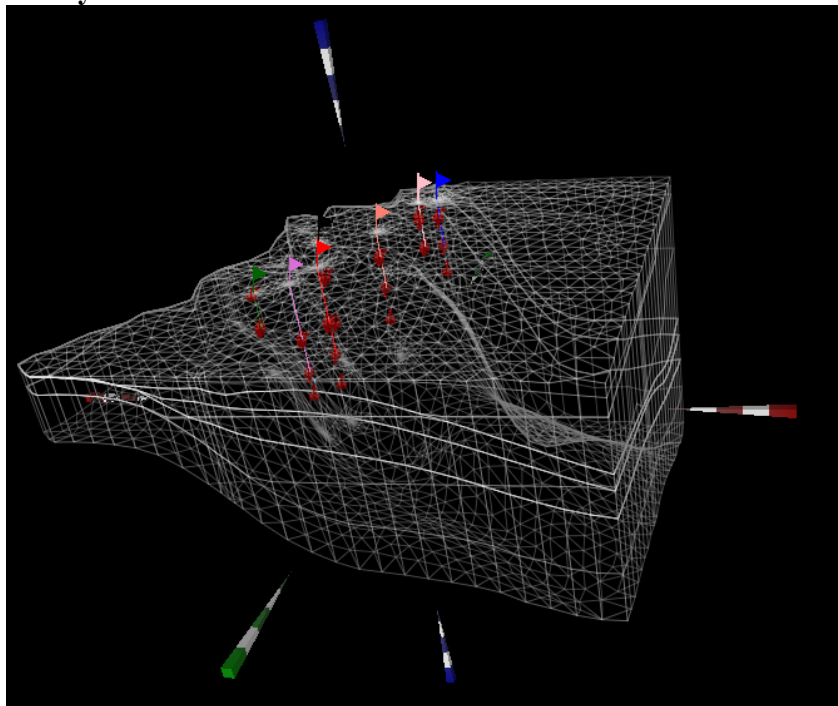
Different combinations of production rates and well rotations were simulated. In order to obtain a sustainable status for water supply, a minimum hydraulic head constraint was set to be the top of the Casper Aquifer at all well locations thus the Casper Aquifer will be under confined condition.

In the first case, a set of target pumping rates were used based on recommendation from [1]. The pumping rates were assigned to all wells, and the simulation results are shown in Table 5. Water level in Duck Creek No.1 Well drops under the minimum water level constraint, thus, Duck Creek No.1 is not suggested to be used as production well even with a relatively small production rate. All wells in Lone Tree Compartment have good potentials to produce.

Table 5: Suggested pumping rate from [1] and simulation results when all wells are pumping using the suggested rate.

	Production rate (gpm)	Minimum water level constraint	Simulated water level
LT1	600	1981.5	2114.05
LT15	600	1935.6	2134.42
LT12	600	1832.4	2142.87
GC22C	100	1556.1	2151.76
DC31	200	1619.7	2144.18
DC1	200	2196.2	2152.18

In the second case, all wells were pumped separately with high production rate (1000 gpm) for 5 years. Water levels of wells in Lone Tree Creek Compartment do not have significant change. In Goose Creek Compartment, water level drops 27 meters in Goose Creek 2-2C. In Duck Creek Compartment, water levels in two wells drop the most comparing to other wells (Table 6).

Table 6: Simulation results for separately pumping events with high production rate.

	Production rate (gpm)	Minimum water level constraint	Simulated water level	Water Level Difference (m)
LT1	1000	1981.5	2114	0.3
LT15	1000	1935.6	2134	0.8
LT12	1000	1832.4	2161	0.9
GC22C	1000	1556.1	2129	27.1
DC31	1000	1619.7	2099	57.9
DC1	1000	2196.2	2096	71.4

In the third case, Lone Tree Fault No.1 and Lone Tree Fault 1-5 wells were pumped simultaneously with production rate of 4000 gpm for 5 years. Water level is not dropping significantly (Table 7).

Table 7: Simulation results for simultaneous pumping events with high production rate for Lone Tree Fault No.1 and Lone Tree Fault 1-5 wells.

	Production rate (gpm)	Minimum water level constraint (m)	Simulated water level (m)	Water Level Difference (m)
LT1	4000	1981.5	2112	2.3
LT15	4000	1935.6	2133	1.8

Based on the above results, candidate wells are the three wells in Lone Tree Creek Compartment. Besides water level, sand production is another factor that needs to be considered

for production wells (Table 8). Among three wells in Lone Tree Compartment, Lone Tree 1-5 has the smallest sand production, thus Lone Tree 1-5 is the best candidate for water production.

Table 8: Sand production rates for 4 wells.

	Sand Production (ppm)
LT1	0.37/0.07
LT15	Trace
LT12	
GC22C	0.01
DC31	0.56
DC1	

<u>Pumping Program:</u>

Based on flow simulation using the 3D groundwater models, a pumping plan has been designed (Table 9), where individual well production rate is selected based on the well capacity and historic precipitation data (Figure 2). Lone Tree Fault No.1 and Lone Tree Fault 1-5 are the two main wells that can be used for water production. This pumping program, however, will be affected by specific precipitation of the year (i.e., future climate condition) and other factors such as sand production.

Table 9: Pumping program for 6 wells in a year.

Pumping Rate	January	February	March	April	May	June	July	August	September	October	November	December
LT1	1000	1000	2000	2000	3000	3000	3000	3000	2000	2000	1000	1000
LT15	1000	1000	2000	2000	3000	3000	3000	3000	2000	2000	1000	1000
LT12	800	800	1500	1500	2000	2000	2000	2000	1500	1500	800	800
GC22C	-	-	200	200	200	200	200	200	200	200	200	-
DC31	-	-	500	500	500	500	500	500	500	500	500	-
DC1	-	-	-	-	-	-	-	-	-	-	-	-

5   Conclusion & Significance

Using a new inverse theory, this research first calibrated a 2D groundwater model for the Casper Aquifer in Belvoir Ranch with sparse hydrological observations. The new theory enables the joint estimation of aquifer hydraulic conductivities and boundary conditions under steady state flow. Water levels of 7 wells in April 2016 were used to condition the inversion, when water levels in all wells were relatively stable compared to other months. By incorporating geophysical and borehole data at the Belvoir Ranch, a 3D aquifer model was built next. Aquifer boundary conditions in April 2016, inverted using the new inverse method, were imported to the model, the assumption being that the radial cone of depression from the pumping program will not reach the actual boundaries. The calibrated hydraulic conductivity values, also obtained from steady-state inversion, were assigned to the Casper Aquifer layers in the 3D model. For the 3D model, hydraulic parameters of multiple hydrogeological units (including the Casper Aquifer) were further calibrated using pumping tests data from 2011. With this model, various design pumping programs (pumping rates and well rotations) were simulated. To select water supply wells among the current 6 test wells, the recommended aquifer compartment is the Lone Tree Compartment of the Casper Aquifer. Lone Tree Compartment not only has the highest hydraulic conductivity, it can also capture the natural recharge into the subsurface from the Lone Tree Fault. Moreover, uncertainties in the model have been reduced using the following strategies: (1) To reduce uncertainty of aquifer

K distribution, the model was divided into zones given the observed geological data, and an equivalent K was estimated for each zone to represent small-scale heterogeneity not incorporated in model. The equivalent Ks were calibrated using both steady state inversion and transient pumping test data; (2) To reduce uncertainty of location, timing, and rate of aquifer recharge, a recharge layer was assigned on the top of the model during both parameter calibration and simulation; (3) To reduce the uncertainty of aquifer boundary conditions, the novel inverse method was used to invert the likely aquifer boundary conditions. Overall, this study has successfully reduced uncertainties in the model, and gives predicted water level responses for future production programs. This research also marks the first successful application of a new groundwater inverse method where aquifer hydraulic parameters and boundary conditions are jointly estimated.

Publications & Presentations:
Fangyu Gao†, Ye Zhang (2018) An inverse method for the simultaneous estimation of aquifer thickness, hydraulic conductivities, and boundary conditions using borehole and hydrodynamic data, Journal of Hydrology, in preparation.

Fangyu Gao†, Ye Zhang (2017) Simultaneous estimation of aquifer thickness, conductivity, and BC using borehole and hydrodynamic data with geostatistical inverse direct method, AGU Annual Meeting, New Orleans, Louisiana, poster presentation.

Fangyu Gao†, Ye Zhang (2017) Applying spectral data analysis techniques to infer aquifer properties in Belvoir Ranch, Wyoming, AGU Annual Meeting, New Orleans, Louisiana, poster presentation.

Fangyu Gao†, Ye Zhang (2017) A new inverse method for the simultaneous estimation of aquifer thickness and boundary conditions based on borehole and hydrodynamic measurements, AGU Hydro Days, Fort Collins, CO, March 20 – 22, 2017, oral presentation.

Student Support:
One student, Miss Fangyu Gao, has been funded by this project since September 2015. Miss Gao received her B.S. and M.S. in Petroleum Engineering from the Colorado School of Mine. She is currently a 3nd year Ph.D. candidate in the Program of Hydrology at the Department of Geology & Geophysics, University of Wyoming. She has successfully completed her Ph.D. Qualifying and Ph.D. Preliminary Exam during the Fall semester of 2016 and Spring semester of 2018. Fangyu is currently writing up her research outcomes in the form of two journal articles.

Conferences Attended:
AGU Annual Meeting, 2016;
AGU Hydrology Days, 2017;
AGU Annual Meeting, 2017.

References Cited:
[1] Lidstone and Associate (2012) Final Report: Cheyenne Belvoir Ranch Groundwater Level II, prepared for: Wyoming Water Development Commission, Cheyenne, Wyoming.
[2] Hermann, R., M. Pearce, K. Burgess, and A. Priestley (2004) Integrated Aquifer Characterization and Numerical Simulation for Aquifer Recharge and Storage at Marco Lakes, Florida, in *Hydrology: Science and Practice for the 21st Century*, Volume I, p. 276-283, published by the British Hydrological Society.

[3] Black, W., M. Dawoud, R. Hermann, D. Largeau, R. Maliva, and R. Will (2008) Managing a Precious Resource, *Oilfield Review,* Summer 2008, a Schlumberger quarterly publication, page 18-33.

[4] Zhang, Y., (2013)a Reducing Uncertainty in Calibrating Aquifer Flow Model with Multiple Scales of Heterogeneity, *Groundwater*, doi: 10.1111/gwat.1211.

[5] Irsa, J. and Y. Zhang (2012) A New Direct Method of Parameter Estimation for Steady State Flow in Heterogeneous Aquifers with Unknown Boundary Conditions, *Water Resources Research*, 48, W09526,DOI:10.1029/2011WR011756

[6] Zhang, Y. (2013)b Nonlinear Inversion of an Unconfined Aquifer: Simulation of Acid Gas Disposal in Western Wyoming, *AAPG Bulletin,* Vol. 96, No. 4, p. 635-664

[7]PEST (Model-Independent Parameter Estimation and Uncertainty Analysis), http://www.pesthomepage.org/Home.php

[8] Cheyenne Climate Overview https://www.bestplaces.net/climate/city/wyoming/cheyenne

[9]McMahon, P.B., Plummer, L.N., Böhlke, J.K., Shapiro, S.D. and Hinkle, S.R., 2011. A comparison of recharge rates in aquifers of the United States based on groundwater-age data. Hydrogeology Journal, 19(4), p.779.